JFM RAPIDS
journals.cambridge.org/rapids

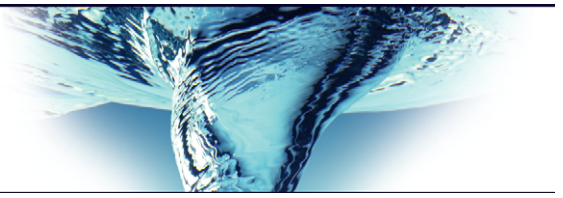

Spontaneous layering in stratified turbulent Taylor–Couette flow

R. L. F. Oglethorpe[1,2,†], C. P. Caulfield[2,1] and Andrew W. Woods[2]

[1]Department of Applied Mathematics and Theoretical Physics, Centre for Mathematical Sciences, University of Cambridge, Wilberforce Road, Cambridge CB3 0WA, UK

[2]BP Institute, University of Cambridge, Madingley Road, Cambridge CB3 0EZ, UK

(Received 17 December 2012; revised 4 February 2013; accepted 6 February 2013; first published online 19 March 2013)

We conduct a series of laboratory experiments to study the mixing of an initially linear stratification in turbulent Taylor–Couette flow. We vary the inner radius, R_1, and rotation rate, Ω, relative to the fixed outer cylinder, of radius R_2, as well as the initial buoyancy frequency $N_0 = \sqrt{(-g/\rho)\partial\rho/\partial z}$. We find that a linear stratification spontaneously splits into a series of layers and interfaces. The characteristic height of these layers is proportional to U_H/N_0, where $U_H = \sqrt{R_1\Delta_R}\Omega$ is a horizontal velocity scale, with $\Delta_R = R_2 - R_1$ the gap width of the annulus. The buoyancy flux through these layers matches the equivalent flux through a two-layer stratification, independently of the height or number of layers. For a strongly stratified flow, the flux tends to an asymptotic constant value, even when multiple layers are present, consistent with Woods *et al.* (*J. Fluid Mech.*, vol. 663, 2010, pp. 347–357). For smaller stratification the flux increases, reaching a maximum just before the layers disappear due to overturning of the interfaces.

Key words: mixing and dispersion, stratified flows, Taylor–Couette flow

1. Introduction

Stably stratified turbulent flows, where the density decreases with height, are common in the environment. In particular, turbulent mixing processes play a key role in the circulation of the ocean (Ivey, Winters & Koseff 2008; Ferrari & Wunsch 2009). Since the buoyancy force in a stably stratified fluid acts as a restoring force on vertical displacement, turbulent mixing requires work to be done against this buoyancy force, and it seems plausible for the stable stratification to reduce vertical fluxes of quantities such as heat and salt.

There have been many experimental studies of the mechanical mixing of an initially two-layer stratification (see, for example, Turner 1968; Linden 1979; Strang

† Email address for correspondence: R.L.F.Oglethorpe@damtp.cam.ac.uk

doi:10.1017/jfm.2013.85

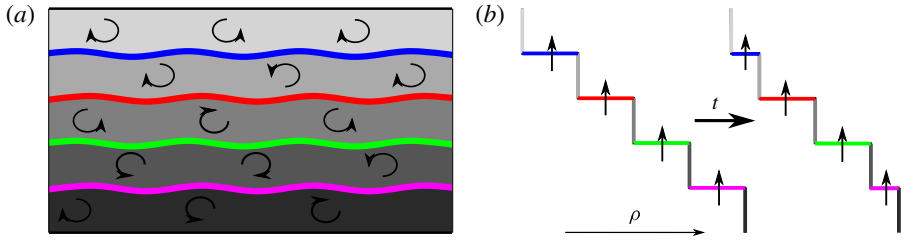

FIGURE 1. (*a*) The mixing process in a multiple-layer stratification, where turbulent eddies in the mixed layers scour either side of the density interfaces. (*b*) The density profile for a multiple-layer stratification, and its variation over time as salt is transported through the interfaces. Over a long period the density differences between the inner layers do not vary.

& Fernando 2001). Woods *et al.* (2010), henceforth referred to as W10, studied the mixing of a two-layer salt stratification in turbulent Taylor–Couette flow. In a two-layer stratification, when there is a high density difference, $\Delta\rho$, between the layers, turbulent mixing is caused by 'scouring' of fluid from either side of the density interface, rather than by turbulent eddies overturning the interface (Kato & Phillips 1969). This scouring initially sharpens the interface, and causes it to remain sharp for most of the experiment (Guyez, Flor & Hopfinger 2007). Over time, $\Delta\rho$ decreases due to mixing by scouring, until $\Delta\rho$ is low enough that turbulent eddies can overturn the interface, and the two layers rapidly merge. W10 found that, for a sufficiently high $\Delta\rho$, the buoyancy flux per unit area through the interface, F, is a non-zero constant, independent of the current value of $\Delta\rho$:

$$F = \frac{\mathrm{d}}{\mathrm{d}t}\int_0^{H/2} \frac{g(\rho(z)-\rho_0)}{\rho_0}\,\mathrm{d}z = -\frac{H}{4}\frac{g}{\rho_0}\frac{\mathrm{d}\Delta\rho}{\mathrm{d}t} \propto \Omega^3, \tag{1.1}$$

where $H/2$ is the height of each layer, g is the acceleration due to gravity, $\rho(z)$ is the density of the fluid, which is close to constant in each layer, ρ_0 is a reference density (using the Boussinesq approximation), and Ω is the rotation rate of the inner cylinder.

This surprising result is in contrast to results from mixing experiments with grid-generated turbulence (Turner 1968; Linden 1979; Zellouf, Dupont & Peerhossaini 2005), where the experimental data suggest that the turbulent flux decays to zero as the strength of the stratification increases. In order to build up our understanding of turbulent mixing in Taylor–Couette flows, we complement the results from W10 by studying the mixing of a stable linear stratification in high-Reynolds-number Taylor–Couette flow, $Re = \Omega R_1 \Delta_R/\nu = O(10^4)$, where R_1 is the radius of the inner cylinder, $\Delta_R = R_2 - R_1$ is the gap width, and ν is the kinematic viscosity.

In different geometries, previous experiments (Ruddick, McDougall & Turner 1989; Park, Whitehead & Gnanadeskian 1994; Holford & Linden 1999) and numerical simulations (Balmforth, Llewellyn Smith & Young 1998; Basak & Sarkar 2006; Brethouwer *et al.* 2007) have found that a linear stratification can spontaneously form into layers and interfaces. Figure 1 shows a cartoon of the turbulent mixing process that we might expect in such a flow with multiple layers. As in a two-layer stratification, we expect a flux of salt upwards through the interfaces by a scouring process, so that the density of the top layer increases and the density of the bottom

layer decreases. However, if the flux through all the interfaces is the same then the density of the interior layers and the density jumps across the interleaving interfaces should remain constant.

Boubnov, Gledzer & Hopfinger (1995) previously found that layers appeared in linearly stratified, low-*Re* Taylor–Couette flow. We are interested in investigating whether layers appear and survive for a long time in our strongly turbulent experiment, and, if so, we wish to find the depth of these layers, whether these interfaces have the same flux properties as the two-layer experiments described in W10, and how the vertical density profiles evolve over time. To investigate these issues, the rest of the paper is organized as follows. In § 2 we describe the experimental method, while in § 3 we describe and discuss our experimental observations. Finally, in § 4 we briefly draw our conclusions.

2. Experiment

Our experiment uses a Taylor–Couette tank similar to that used by W10. The outer cylinder has an internal radius of 25.7 cm, and we use three different inner cylinders, with radii of 5, 10 and 15 cm. The outer cylinder and base are stationary, while the top surface of the fluid is a free surface. The flow is driven by the rotation of the inner cylinder, which has a range of angular velocities from 5 to 24 r.p.m (0.5 to 2.5 rad s^{-1}). We fill the tank with an initially linear stratification (ILS) of salt, using the double bucket method originally described by Oster (1965). In addition, we also conduct experiments using an initially layered stratification, either initially two-layer (ITL), as in W10, or initially five-layer (IFL), where each layer is of equal depth. In all cases, we fill the tank through a sponge to minimize mixing during the filling process. The total height of fluid in the tank ranges from 27.5 to 48.9 cm.

A conductivity probe, mounted on a traverse above the tank, takes continuous vertical density profile measurements. We calibrate the conductivity probe before each experiment using up to six samples of different salinity. We only use data from the downwards moving profile, since the probe measures its own wake while it is moving upwards, and this gives one profile approximately every two minutes. We assume that the profiles are the same over the horizontal area of the annulus, and we check this by visual observation during the experiment. The conductivity probe siphons fluid out of the tank at a rate of approximately 1.2×10^{-7} m^3 s^{-1}, causing the top surface to move down at a rate of up to 10^{-6} m s^{-1}, and giving a change in total height of 1–3 cm over the course of an experiment. This can be neglected in ITL experiments (as in W10), but must be taken into account in ILS experiments, where layer heights can be of a comparable size to this change in height due to siphoning.

3. Observations

Consistently with the previous experiments mentioned in the Introduction, we find that an ILS experiment spontaneously forms into layers separated by sharp interfaces. Figure 2 shows the evolution of the vertical density profiles over time for two different ILS experiments. The interfaces, which are identified as local maxima of $|\partial\rho/\partial z|$, are shown as black lines, and appear to have an approximately constant thickness $l_i \approx 1$ cm, consistently with many other studies (e.g. Crapper & Linden 1974; Shravat, Cenedese & Caulfield 2012). The layers and interfaces appear to be long-lived, which suggests that they are not simply a spin-up effect, and the layers appear to have a characteristic height, h_l, which varies with Ω, R_1 and the initial buoyancy

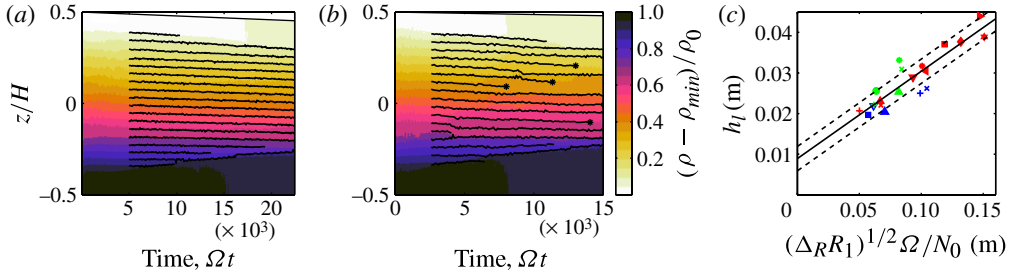

FIGURE 2. Variation of density profiles over time for two ILS experiments, and their interfaces (solid black lines): (*a*) $R_1 = 10$ cm, $N_0 = 1.58$ s^{-1}, $\Omega = 0.73$ rad s^{-1}; (*b*) $R_1 = 10$ cm, $N_0 = 1.54$ s^{-1}, $\Omega = 0.95$ rad s^{-1}. Asterisks in (*b*) indicate layer coarsening, when interior interfaces are overturned. (*c*) Early-time layer heights for ILS experiments, varying Ω and N_0, for $R_1 = 5$ cm (blue), $R_1 = 10$ cm (red), $R_1 = 15$ cm (green), with a linear fit to the data (solid line) and one standard deviation from the linear fit (dashed line).

frequency $N_0 = \sqrt{(-g/\rho)\partial\rho/\partial z}$. The range of Taylor numbers in our experiments, $1.8 \times 10^4 T_c \leqslant Ta \leqslant 1.5 \times 10^5 T_c$, where $Ta = 2R_1^2\Delta_R^3\Omega^2/(R_2 + R_1)^2\nu^2$ and T_c is the critical Taylor number for instability (Roberts 1965), is sufficiently high that in an unstratified flow we might expect a series of turbulent Taylor vortices with height $h \sim \Delta_R$ (Koschmeider 1979). The layers we observe in an ILS experiment do not appear to be associated with unstratified turbulent Taylor vortices, since they are significantly smaller than Δ_R, and strongly depend on the stratification and rotation rate.

In figure 2, N_0 is similar for the two experiments, but Ω is higher for the experiment in figure 2(*b*) than in figure 2(*a*). Correspondingly, the layers are larger in figure 2(*b*) than in figure 2(*a*). The layers are eroded from the top and bottom, and the interior layers also appear to coarsen over time, when the density difference across an interface decays until it is low enough for the interface to overturn (marked by the asterisks in figure 2*b*). The interfaces also have an overall drift downwards over time, due to the removal of fluid from below the interfaces by the probe, as mentioned above. As the layers coarsen, they may become of the same scale as the unstratified Taylor vortices. We will focus only on the behaviour of the early layers, when the interior layers remain at the height h_l associated with the stratification. During this stage, the density of the interior layers and the density jumps across the interior interfaces remain approximately constant, consistently with the schematic presented in figure 1.

3.1. *Layer heights*

We conduct a series of experiments to test how the average height of the early layers, h_l (defined as the distance between the centre of adjacent interfaces), varies with Ω, R_1 and N_0. Boubnov *et al.* (1995) suggested a possible energy argument for the height of the early layers. In Taylor–Couette flow, when a fluid parcel moves away from the inner cylinder, the centrifugal force, Φ_{cf},

$$\Phi_{cf} = \frac{u_\theta^2}{r} \propto R_1\Omega^2 \quad \text{at } r = R_1, \tag{3.1}$$

does work against the radial pressure gradient. When the fluid parcel has moved a distance Δ_R to the outer cylinder, the work done is $W = \Delta_R \Phi_{cf} \propto \Delta_R R_1 \Omega^2$.

The work to raise the fluid element a height h in a linear stratification with buoyancy frequency N_0 is $W = N_0^2 h^2$, and the maximum height is reached when all the work is put into raising the fluid, giving

$$\Delta_R R_1 \Omega^2 \propto N_0^2 h^2 \Rightarrow h \propto \sqrt{\Delta_R R_1}\frac{\Omega}{N_0} = \frac{U_H}{N_0}, \tag{3.2}$$

where $U_H = \sqrt{\Delta_R R_1}\Omega$ is a horizontal velocity scale. The data are consistent with this scaling for the early layer height, which also agrees with results from Park *et al.* (1994) and Holford & Linden (1999). Figure 2(*c*) shows how h_l (the time-average of the layer depth over the period between the initial identification of interfaces and the first disappearance of an interface) varies with U_H/N_0, with a linear fit of

$$h_l = \left(0.215\frac{U_H}{N_0} + 0.009\right) \pm 0.003 \text{ m} \approx A\frac{U_H}{N_0} + c, \tag{3.3}$$

where the error is one standard deviation from the linear fit. The y-intercept is non-zero because h_l includes both the spacing between the interfaces and the interface thickness, which is typically $O(1)$ cm. Figure 2(*c*) shows some scatter, which is partly due to quantization effects and partly due to inherent turbulent flow randomness during layer formation. Although we are not able to measure the dissipation rate $\mathscr{E}$ directly, the scaling (3.3) also suggests that the buoyancy Reynolds number, $Re_b = \mathscr{E}/\nu N_0^2$ is sufficiently large in our experiments for the flow to be in the 'stratified turbulence' regime (Brethouwer *et al.* 2007), so that mixing occurs even when the flow is very strongly stratified (Wells, Cenedese & Caulfield 2010).

3.2. *Buoyancy flux*

We now wish to compare the flux through each spontaneously formed interface in an ILS experiment with the flux through an ITL stratification, for varying Ω and R_1. We construct a scaling for F (defined in (1.1)) by considering the kinetic and potential energy densities in an ITL stratification. For an ITL stratification, with layers of equal height $H/2$, we define the potential energy density as

$$\mathscr{P} = \frac{1}{\rho_0 H}\int_{-H/2}^{H/2} \rho(z,t) g z \,\mathrm{d}z = -\frac{gH\Delta\rho}{8\rho_0}, \quad \frac{\mathrm{d}\mathscr{P}}{\mathrm{d}t} = -\frac{Hg}{8\rho_0}\frac{\mathrm{d}\Delta\rho}{\mathrm{d}t}, \tag{3.4}$$

noting that $\mathrm{d}\Delta\rho/\mathrm{d}t < 0$ and $\mathscr{P}$ increases with time.

The kinetic energy is supplied to the fluid by shear at the inner cylinder, so we assume that the characteristic energy injection velocity scale is $U_{\mathscr{K}} \propto R_1\Omega$ and that the characteristic length scale for energy dissipation is the gap width between the cylinders, $L_{\mathscr{K}} = \Delta_R$. On dimensional grounds (following Shravat *et al.* 2012) we assume the dissipation rate $\mathscr{E} \sim U_{\mathscr{K}}^3/L_{\mathscr{K}}$, and we further assume that, in the W10 regime, the rate of increase of $\mathscr{P}$ is a constant fraction of $\mathscr{E}$, following Osborn (1980),

$$\frac{\mathrm{d}}{\mathrm{d}t}\mathscr{P} = \Gamma\mathscr{E}, \quad \mathscr{E} \sim \frac{U_{\mathscr{K}}^3}{L_{\mathscr{K}}} = \frac{C_\epsilon\,(\Omega R_1)^3}{\Delta_R}, \tag{3.5}$$

where C_ϵ is an (undetermined) empirical constant and Γ is assumed a constant. We find that these assumptions lead to a scaling for the buoyancy flux, consistent with

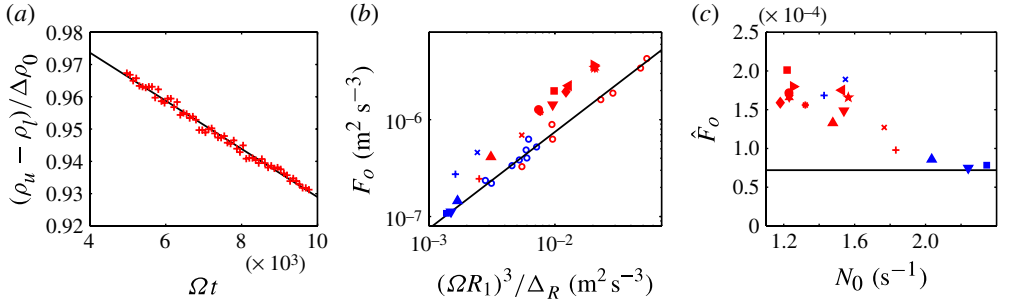

FIGURE 3. (*a*) Variation of $\Delta\rho$ with time for an ILS experiment ($R_1 = 10$ cm, $N_0 = 1.58$ s^{-1}, $\Omega = 0.73$ rad s^{-1}). (*b*) Variation of F_o (defined in (3.7)) with $(\Omega R_1)^3/\Delta_R$ for ILS experiments (filled symbols), compared with the W10 asymptotic regime (black line) and ITL experiments (open circles), for $R_1 = 10$ cm (red) and $R_1 = 15$ cm (blue). (*c*) Variation of $\hat{F}_o$ with N_0 (filled symbols, as in *b*), compared with the W10 asymptotic regime (black line).

the W10 scaling ($F \propto \Omega^3$), with which we define a non-dimensional buoyancy flux $\hat{F}$,

$$F = \frac{1}{4}\frac{\mathrm{d}}{\mathrm{d}t}\left(-\frac{gH\Delta\rho}{\rho_0}\right) = \frac{2\Gamma C_\epsilon (\Omega R_1)^3}{\Delta_R}, \quad \hat{F} = \frac{\Delta_R}{(\Omega R_1)^3}F. \tag{3.6}$$

After a linear stratification has spontaneously formed into layers, the density of the top layer increases and the density of the bottom layer decreases, as in the ITL experiments conducted by W10, while the interior layers remain at a constant density. This suggests that the vertical buoyancy flux through each interface is the same, so that we can characterize the total flux through the stratification by the rate of change of the density difference between the top and bottom layer, $\Delta\rho = \rho_b - \rho_t$, where ρ_t and ρ_b are the densities of the top and bottom layer, respectively. Figure 3(*a*) shows the evolution of $\Delta\rho$ with time for one ILS experiment during the early layers stage, during which $\Delta\rho(t)$ appears to decrease at a constant rate. For comparison with ITL experiments, we define an overall flux, F_o, and non-dimensional flux, $\hat{F}_o$ (see (3.6)), as

$$F_o = -\frac{\overline{H}}{2}\frac{g}{\rho_0}\frac{\mathrm{d}\Delta\rho}{\mathrm{d}t}, \quad \hat{F}_o = \frac{\Delta_R}{(\Omega R_1)^3}F_o, \tag{3.7}$$

where $\overline{H}$ is the average height of the top and bottom layers. For an ITL stratification, $F_o = F$ as defined in (1.1). During the early layers stage, F_o appears to be constant. Figure 3(*b*) shows the variation of constant F_o with $(\Omega R_1)^3/\Delta_R$ for several ILS experiments, compared with F_o for an ITL stratification in the W10 'asymptotic regime', which we also found for our tank by considering strongly stratified ITL experiments. In most of the ILS experiments, the flux through the spontaneously formed interfaces appears to be higher than the W10 scaling, although three of the ILS experiments do show a consistent scaling with the ITL asymptotic regime.

In the W10 asymptotic regime for an ITL stratification, $\hat{F}_o$ is a constant, independent of the current value of $\Delta\rho$, provided that $\Delta\rho$ is sufficiently high. Figure 3(*c*) shows the variation of $\hat{F}_o$ with N_0, compared with the constant $\hat{F}_o$ expected from the W10 scaling. The flux agrees with the W10 scaling at sufficiently high N_0, and appears to increase as N_0 decreases; indeed, for most of these ILS experiments,

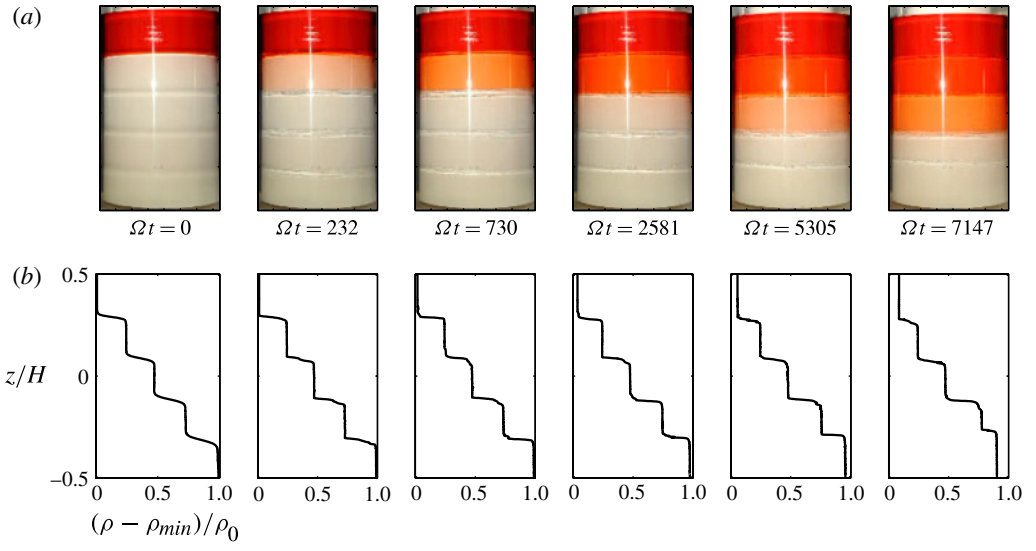

FIGURE 4. Time series of (*a*) photos of an artificial layer experiment with an initially dyed top layer and (*b*) corresponding density profiles ($R_1 = 15$ cm, $\Omega = 0.83$ rad s^{-1}).

the density difference across each of the spontaneously formed interfaces, $\Delta\rho_i$, seems to be too low (in some sense) for the interfaces to be in the W10 asymptotic regime. The scatter in figure 3(*c*) is due both to the variation in Ω, which leads to different layer heights and thus different $\Delta\rho_i$, and to turbulent fluctuations, as in figure 2(*c*). The early layers that form in an ILS experiment are also observed to be evenly spaced, and if we assume that $h_l > 2l_i$ for the layered structure to be distinguishable, where l_i is the interface thickness, then

$$\frac{h_l}{H} \approx \frac{\Delta\rho_i}{\Delta\rho} = \frac{g}{\rho_0}\frac{\Delta\rho_i}{N_0^2 H}, \quad \frac{g}{\rho_0}\Delta\rho_i \approx N_0^2 h_l < \frac{2A^2 U_H^2 l_i}{(2l_i - c)^2} \approx \frac{2A^2 U_H^2}{l_i}, \tag{3.8}$$

where $\Delta\rho_i$ is the density difference across each interface, $A \approx 0.2$ and $c \approx 1$ cm are empirical constants defined by $h_l \approx AU_H/N_0 + c$ (see (3.3)), and $l_i \approx 1$ cm. Thus $\Delta\rho_i$ is limited by U_H, which depends on the geometry of the tank, a point we return to in § 3.5. Although it is possible for ILS experiments to have $\Delta\rho_i$ sufficiently large to be in the W10 asymptotic regime, it is more convenient to start an experiment with an initially layered stratification, with multiple layers each of height larger than h_l, with $\Delta\rho_i$ chosen to be sufficiently large to be in the W10 asymptotic regime.

3.3. *Initially five-layer experiments*

Figure 4 shows the evolution over time of such an experiment with an initially five-layer (IFL) density stratification. (The heights of these layers are approximately four times the height, h_l, of the layers that would spontaneously form in an equivalent ILS experiment.) As with the layers and interfaces formed in an ILS experiment, we observe stationary interfaces and well-mixed layers. Also, as in an ILS experiment, the densities of the outer layers evolve over time, while the interior layers remain at a constant density. In figure 4, the top layer was initially dyed red. We observe that over

time the dye is transported into the lower layers, through the interfaces. There also appears to be some interface sharpening between the first density profile (immediately before the start of the experiment) and the second density profile (after approximately 40 rotations), and some upwards erosion of the bottom interface.

3.4. *Flux through interior interfaces*

In a stratification with multiple layers and interfaces, salt is simultaneously transported into a layer through its bottom interface and out of a layer through its top interface. We define the mass above an interface and flux through an interface, at height h, time t, as

$$M(h,t)=\sum_{j=1}^{n} H_j(t)\rho_j(t), \quad F_l(h,t)=\frac{g}{\rho_0}\frac{\mathrm{d}}{\mathrm{d}t}M(h,t), \tag{3.9}$$

where there are n layers above the interface, and $H_j(t)$ and $\rho_j(t)$ are the height and density of layer j above the interface, respectively. For an ITL stratification with layers of equal height $H/2$, $F_l=F=F_o$, as defined in (1.1) and (3.7).

In an ILS experiment, we find that the interfaces do not always remain at a constant height, but can migrate over time (see figure 2). We modify F_l in (3.9) to remove the effects of siphoning by the probe and of interface migration (Shravat *et al.* 2012). The total dimensional and non-dimensional turbulent entrainment flux, F_e and $\hat{F}_e$, are then given by

$$F_e(h,t)=\frac{(\Omega R_1)^3}{\Delta_R}\hat{F}_e=\frac{g}{\rho_0}\left(\frac{\mathrm{d}}{\mathrm{d}t}[M(h,t)+m_p(h,t)]+\left[\frac{\mathrm{d}h}{\mathrm{d}t}-\frac{\mathrm{d}h_p}{\mathrm{d}t}\right]\rho(h,t)\right), \tag{3.10}$$

respectively. The first pair of terms on the right-hand side gives the total rate of change of mass above the interface, both the observed mass, M, and the mass removed by the probe, m_p. The second pair of terms is an adjustment to remove the effects of interface migration, where the height of the interface changes at an observed rate of $\mathrm{d}h/\mathrm{d}t$. The migration appears to be partly due to the probe, which removes fluid from beneath the interface and causes the interface to move downwards at a rate $\mathrm{d}h_p/\mathrm{d}t$. Remaining migration is due to the top and bottom boundaries, since without these we would expect an equal amount of turbulent entrainment on either side of each interface, and the interface to remain at a constant height. When interface migration occurs due to the top and bottom boundaries, fluid moves from one side of the interface to the other, adding an extra mass flux which is not due to turbulent entrainment.

For an ITL stratification with layers of equal size (as in W10), there is no interface migration and $\mathrm{d}h_p/\mathrm{d}t$ and $\mathrm{d}m_p/\mathrm{d}t$ are negligible. In this case, $F_e=F=F_o=F_l$ as defined in (1.1), (3.7) and (3.9). For the interfaces in an ILS experiment, in order to reduce error, we find the flux through an interface, F_e, as an average value over the early layers stage, during which the flux is approximately constant (see figure 3*a*), rather than as an instantaneous measurement.

3.5. *Universal flux law*

For an ITL stratification, we define a Richardson number as $Ri=g\Delta\rho D/(\rho_0 u^2)$, following W10, where D is a length scale and u is a characteristic velocity of the turbulent flow. We assume that the characteristic u is governed by the speed of the inner cylinder, consistently with the particle image velocimetry measurements in W10, so that $u\propto R_1\Omega$ (note that this velocity is different from the velocity U_H used in (3.3)).

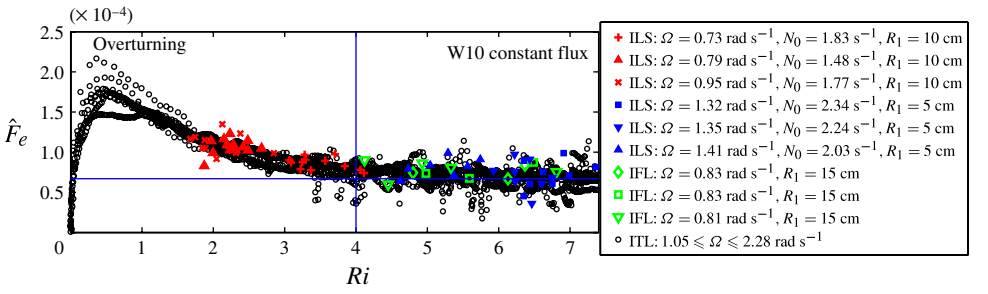

FIGURE 5. Non-dimensional flux $\hat{F}_e$ (defined in (3.10)) through individual interfaces: six ILS experiments (filled coloured symbols, corresponding to figure 3); three IFL experiments (open green symbols); 12 ITL experiments with varying R_1, Ω and initial $\Delta\rho$ (open black circles). Each coloured symbol represents a different interface in one experiment. The solid blue lines show the constant $\hat{F}_e$ in the W10 asymptotic regime and the empirical value of Ri_a.

One might expect the length scale D to be either the height of the layers or the gap width Δ_R, since these could limit the size of the turbulent eddies in the layers. However, we find empirically that the results from an ITL stratification for various inner cylinders show the best collapse when D is taken as a constant. We take $D \propto R_2$, since this is the only constant external length scale in our experiments, and our empirical Ri, for layered and linear stratifications, respectively, becomes

$$Ri = \frac{g\Delta\rho}{\rho_0}\frac{R_2}{(R_1\Omega)^2}, \quad Ri = \frac{R_2 N_0}{(R_1\Omega)^2}(AU_H + cN_0). \tag{3.11}$$

This Richardson number quantifies the strength of the stratification, with $\Delta\rho = \Delta\rho_i$ for each interface in a stratification with multiple layers and interfaces.

Figure 5 shows the variation of the flux $\hat{F}_e$ with Ri for individual interfaces (for any ITL experiment, time increases from right to left). The fluxes appear to collapse onto the same non-monotonic curve, which suggests that $\hat{F}_e$ is independent of the height and number of layers. Furthermore, this collapse suggests that the dissipation length scale, $L_{\mathscr{K}}$ (see (3.5)), does not depend on h_l, and that the scouring of the interfaces is therefore a very horizontally localized process. For any type of initial stratification, we find that the flux through an interface is constant for $Ri > 4$, independent of the current value of $\Delta\rho_i$, so that the lower limit of the W10 asymptotic regime is empirically at $Ri = Ri_a \approx 4$. Using (3.8), we now expect the spontaneously formed interfaces with $R_1 = 10$ cm or $R_1 = 15$ cm to always have Ri smaller than this critical value, since

$$Ri_{max} \approx \frac{2A^2U_H^2R_2}{l_i\,(R_1\Omega)^2} = 2A^2(\Delta_R R_2)/(l_i R_1) \approx 3.7, \tag{3.12}$$

where $l_i \approx 1$ cm is the interface thickness. However, for $R_1 = 5$ cm, $Ri_{max} \approx 9.8$, so in this case it is possible for an ILS to form spontaneous layers and interfaces with $Ri > Ri_a$ (as shown in figure 5, consistently with the blue points marked on figure 3*c*). Scatter in Ri for each ILS experiment in figure 5 is due to turbulent fluctuations during layer formation. We have extended the W10 asymptotic regime to $Ri \approx 20$ for ITL experiments, which is not shown in figure 5; however, it is of course possible that the

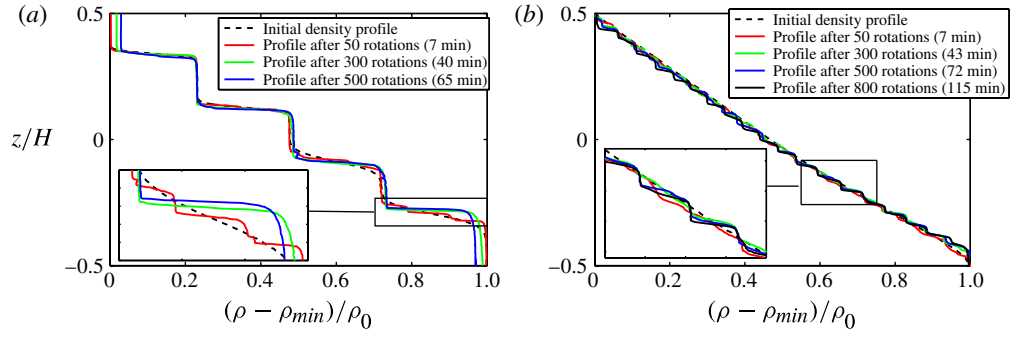

FIGURE 6. Density profiles near the start of an experiment: (*a*) IFL ($R_1 = 15$ cm, $\Omega = 0.83$ rad s^{-1}); (*b*) ILS ($R_1 = 10$ cm, $N_0 = 1.58$ s^{-1}, $\Omega = 0.73$ rad s^{-1}). Insets: details of interface sharpening and layer formation.

behaviour of the flux with Ri may change for very high Ri (see Wells *et al.* 2010 for further discussion of the potential existence of such a regime).

For $0.5 \lesssim Ri \lesssim 4$, the flux increases with decreasing Ri, as expected from figure 3(*c*). In this regime, any small perturbation to a linear density profile is amplified until the density profile forms a step-like structure (Phillips 1972; Posmentier 1977; Park *et al.* 1994; Balmforth *et al.* 1998). The non-monotonic $\hat{F}_e$–Ri relationship shown in figure 5 suggests that an ILS experiment forms layers due to this 'Phillips mechanism'. At $Ri = Ri_c \approx 0.5$, the flux reaches a maximum, two to three times the asymptotic value. Here, $\Delta\rho_i$ is low enough for the interface to overturn; the layers either side of the interface rapidly merge and the flux decreases to zero with decreasing Ri. The large scatter around Ri_c is due to layer merger, which is not yet well understood. Indeed, the value of Ri_c may also vary for the different interfaces in an ILS experiment.

The 'Phillips mechanism' also manifests itself through a sharpening of the interfaces. We illustrate interfacial sharpening for an IFL experiment and spontaneous layer formation for an ILS experiment in figure 6. In figure 6(*a*), the bottom two interfaces were allowed to thicken by diffusion before the start of the experiment. At the start of the experiment, the interfaces sharpen by scouring (as in W10 and Guyez *et al.* 2007 for an ITL stratification). The bottom interface splits spontaneously into several interfaces, each with a low $\Delta\rho_i$. The $\Delta\rho_i$ are different, so the flux through each interface is not balanced, and the interfaces decay to form one single interface with high $\Delta\rho_i$. This sharpening appears to be the same process as the initial formation of layers in an ILS experiment, shown in figure 6(*b*). An ILS experiment spontaneously forms several interfaces, which remain sharp by scouring, with the spacing between them given by h_l (see (3.3)). However, the interfaces formed in an ILS experiment all have approximately the same $\Delta\rho_i$, and so approximately the same flux, and the interfaces are long-lived.

4. Conclusions

Our experiments show that, in turbulent Taylor–Couette flow, an ILS experiment spontaneously forms a series of well-mixed layers and sharp interfaces. The layers have a characteristic height $h_l \propto U_H/N_0 + c$, as defined in (3.3). The vertical buoyancy flux through each interface appears to have the same constant value; when $Ri < Ri_a$,

the flux is higher than the flux expected from the W10 'asymptotic regime', in agreement with our ITL experiments. Figure 5 suggests that, at least for $20 \gtrsim Ri \gtrsim 2$, the flux curve is universal for our experimental parameters, independent of the height and number of layers, and independent of whether the stratification is initially linear or initially layered. The non-monotonicity leads to layer formation by the Phillips mechanism, which appears to be closely related to the sharpening of interfaces by scouring.

Several open questions remain. In particular: what determines the two critical values of Ri, both of which appear to be independent of N_0, Ω, R_1 and Δ_R (and hence the flow Re), i.e. the smaller Ri_c (below which the interface overturns) and the larger Ri_a (above which the flux is constant); what is the spatial distribution of the scouring in the vicinity of interfaces; what determines the length scale embedded in Ri and the (apparently approximately constant) interface thickness l_i, which leads to our measurement of quasi-steady asymptotic finite fluxes; and how do the random turbulent fluctuations affect the layer formation and merger processes? We hope to develop theoretical models to address at least some of these questions, and report on these models in due course.

Acknowledgements

This work has been funded through the BP Institute and EPSRC. Preliminary experiments demonstrating spontaneous layering in initially linearly stratified turbulent Taylor–Couette flow were conducted in 2010 by Clément Saint-Jalm (École Polytechnique) as part of his 'stage de recherche' conducted at the BP Institute under the supervision of C. P. C. and A. W. W. A. Pluck, Dr L. Gladstone, Dr C. Richardson (BPI) and Dr S. B. Dalziel (DAMTP) provided valuable experimental and technical support.

References

BALMFORTH, N. J., LLEWELLYN SMITH, S. G. & YOUNG, W. R. 1998 Dynamics of interfaces and layers in a stratified turbulent fluid. *J. Fluid Mech.* **355**, 329–358.

BASAK, S. & SARKAR, S. 2006 Dynamics of a stratified shear layer with horizontal shear. *J. Fluid Mech.* **568**, 19–54.

BOUBNOV, B. M., GLEDZER, E. B. & HOPFINGER, E. J. 1995 Stratified circular Couette flow: instability and flow regimes. *J. Fluid Mech.* **292**, 333–358.

BRETHOUWER, G., BILLANT, P., LINDBORG, E. & CHOMAZ, J.-M. 2007 Scaling analysis and simulation of strongly stratified turbulent flows. *J. Fluid Mech.* **585**, 343–368.

CRAPPER, P. F. & LINDEN, P. F. 1974 The structure of turbulent density interfaces. *J. Fluid Mech.* **65**, 45–63.

FERRARI, R. & WUNSCH, C. 2009 Ocean circulation kinetic energy: reservoirs, sources and sinks. *Annu. Rev. Fluid Mech.* **41**, 253–282.

GUYEZ, E., FLOR, J.-B. & HOPFINGER, E. J. 2007 Turbulent mixing at a stable density interface: the variation of the buoyancy flux-gradient relation. *J. Fluid Mech.* **577**, 127–136.

HOLFORD, J. M. & LINDEN, P. F. 1999 Turbulent mixing in a stratified fluid. *Dyn. Atmos. Oceans* **30**, 173–198.

IVEY, G. N., WINTERS, K. B. & KOSEFF, J. R. 2008 Density stratification, turbulence, but how much mixing. *Annu. Rev. Fluid Mech.* **40**, 169–184.

KATO, H. & PHILLIPS, O. M. 1969 On the penetration of a turbulent layer into stratified fluid. *J. Fluid Mech.* **37**, 643–655.

KOSCHMEIDER, E. L. 1979 Turbulent Taylor vortex flow. *J. Fluid Mech.* **93**, 515–527.

LINDEN, P. F. 1979 Mixing in stratified fluids. *Geophys. Astrophys. Fluid Dyn.* **13**, 3–23.

OSBORN, T. R. 1980 Estimates of the local rate of vertical diffusion from dissipation measurements. *J. Phys. Oceanogr.* **10**, 83–89.

OSTER, G. 1965 Density gradients. *Sci. Am.* **213**, 70–76.

PARK, Y.-G., WHITEHEAD, J. A. & GNANADESKIAN, A. 1994 Turbulent mixing in stratified fluids: layer formation and energetics. *J. Fluid Mech.* **279**, 279–311.

PHILLIPS, O. M. 1972 Turbulence in a strongly stratified fluid - is it unstable? *Deep-Sea Res.* **19**, 79–81.

POSMENTIER, E. S. 1977 The generation of salinity fine structure by vertical diffusion. *J. Phys. Oceanogr.* **7**, 298–300.

ROBERTS, P. H. 1965 Appendix: The solution of the characteristic value problems. *Proc. R. Soc. Lond.* A **283**, 550–555.

RUDDICK, B. R., MCDOUGALL, T. J. & TURNER, J. S. 1989 The formation of layers in a uniformly stirred density gradient. *Deep-Sea Res.* **36**, 597–609.

SHRAVAT, A., CENEDESE, C. & CAULFIELD, C. P. 2012 Entrainment and mixing dynamics of surface-stress-driven stratified flow in a cylinder. *J. Fluid Mech.* **691**, 498–517.

STRANG, E. J. & FERNANDO, H. J. S. 2001 Entrainment and mixing in stratified shear flows. *J. Fluid Mech.* **428**, 349–386.

TURNER, J. S. 1968 The influence of molecular diffusivity on turbulent entrainment across a density interface. *J. Fluid Mech.* **33**, 639–656.

WELLS, M., CENEDESE, C. & CAULFIELD, C. P. 2010 The relationship between flux coefficient and entrainment ratio in density currents. *J. Phys. Oceanogr.* **40**, 2713–2727.

WOODS, A. W., CAULFIELD, C. P., LANDEL, J. R. & KUESTERS, A 2010 Non-invasive turbulent mixing across a density interface in a turbulent Taylor–Couette flow. *J. Fluid Mech.* **663**, 347–357.

ZELLOUF, Y., DUPONT, P. & PEERHOSSAINI, H. 2005 Heat and mass fluxes across density interfaces in a grid-generated turbulence. *Intl J. Heat Mass Transfer* **48**, 3722–3735.